# Transient CFD and experimental analysis for improved Pelton turbine casing designs

**S Petley, G A Aggidis**

Lancaster University Renewable Energy Group and Fluid Machinery Group, Engineering Department, Lancaster University, Lancaster, LA1 4YR, UK

Corresponding author: g.aggidis@lancaster.ac.uk (G A Aggidis)

**Abstract**. Impulse turbine casings play a very important role and experience dictates that the efficiency of a Pelton turbine is closely dependent on the success of keeping vagrant spray water away from the turbine runner and the water jet. Despite this overarching purpose, there is no standard design guidelines and casing styles vary from manufacturer to manufacturer, often incorporating a considerable number of shrouds and baffles to direct the flow of water into the tailrace with minimal interference with the aforementioned. Secondly, the success of a casing design is dependent on its ability to maintain this objective across a wide range of operating conditions that vary as a consequence of fluctuations in speed and load, resulting in considerable differences in spray leaving the runner. Conventionally, the baffle plates are designed to be most effective at the best efficiency, or duty, point and have been shown to be ineffective at extremes of speed and load. Therefore, efforts to design a casing with minimal amount of shrouding to reduce manufacturing costs is the objective of the project sponsors. The present work incorporates the Reynolds-averaged Navier Stokes (RANS) k-ε turbulence model and a two-phase Volume of Fluid (VOF) model, using the ANSYS® FLUENT® code to simulate the casing flow in a 2-jet horizontal axis Pelton turbine. The results of the simulation of two casing configurations are compared against flow visualisations and measurements obtained from a model established at the National Technical University of Athens. The CFD simulation also informs the design of new casing inserts to see their influence on the flow. Therefore, the outcome of this investigation provides further insight into guidelines for improved Pelton turbine casing design.

## 1. Introduction

The casing of a Pelton turbine is an important component as it collects the water leaving the runner. Some of this water generates splashing and spray, which may cause interference with the runner and water jet, thereby reducing the efficiency. Therefore the design of the casing as a means to reduce this impact is of interest to manufactures [1].

In recent decades, numerical tools such as Computational Fluid Dynamics (CFD) have been applied to the development of Pelton turbines, more specifically the individual components are treated in isolation and the resulting high fidelity models offer a good prediction of the reasonable gains in efficiency from the optimisation of each component. To date, CFD has been used to analyse and further develop the injector and runner design leading to noticeable improvements, however analysis of the flow within the casing remains complex and as such there are no available studies in the public domain,

documenting how Eulerian mesh based CFD solvers can be used for this task, highlighting the knowledge gap and novelty of this research.

As an alternative approach, some researchers have developed Lagrangian particle based methods. Neuhauser et al. [2] and Rentschler et al. [3], both of Andritz Hydro, documented how the in-house SPH-ALE solver can be used to model the free surface flow in the casing of a Pelton turbine, with the aim of evaluating the potential for improvement of efficiency by additional casing components in rehabilitation projects. However, they note it has taken 12 years to develop the code. Moreover, thanks to the recent improvement in computer hardware, larger two-phase unsteady models can be studied in shorter timescales.

On the basis of the above considerations, this paper will demonstrate how the Reynolds-averaged Navier Stokes (RANS) k-ε turbulence model and a two-phase Volume of Fluid (VOF) model within the ANSYS® FLUENT® code can be employed as a visualisation tool to investigate casing flows and improve the design of a 2-jet horizontal axis Pelton turbine.

Initial experimental measurements were carried out at the at the Laboratory for Hydraulic Machines, National Technical University of Athens (NTUA) and are outlined in Section 2.

## 2. Experimental Results

The experimental results were carried out using the Pelton test rig at NTUA, shown in Figure 1. A high head adjustable speed multistage pump of nominal operation point Q=290 $m^3$/hr, H=130 mWG, coupled via a hydraulic coupler to a 200 kW induction motor is used to feed the model turbine, pumping from the 320 $m^3$ main reservoir of the lab. The tests were carried out using the twin jet Z120 Pelton manufactured by Gilbert Gilkes & Gordon Ltd, which was coupled to a 75kW DC generator with continuous speed regulation.

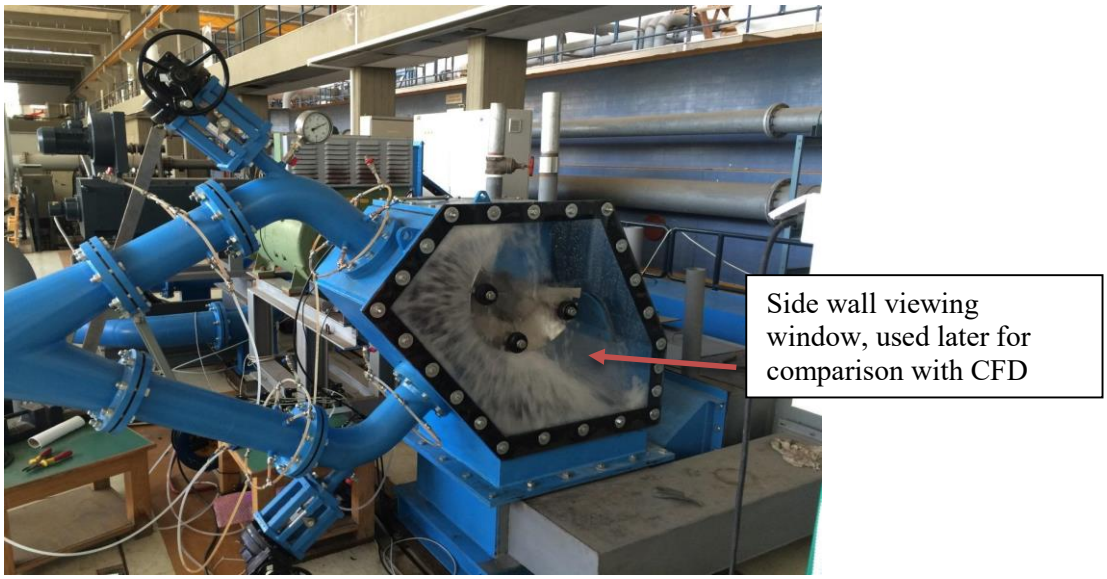


**Figure 1.** Pelton testing facility at NTUA.

Testing and calibration of all the sensors was carried out according to testing standard *IEC 60193* [4] The characteristic equations of turbine unit speed, $n_{11}$, and unit flow, $Q_{11k}$, used to define the operation and performance of the turbine, are given in (1) – (5) below.

$$n_{11} = \frac{n \times D}{\sqrt{H}} \qquad (1)$$

$$Q_{11k} = \frac{Q/N_j}{B^2 \times \sqrt{H}} \quad (2)$$

$$P_{out} = M\omega \quad (3)$$

$$P_{in} = \rho g H Q \quad (4)$$

$$\eta = \frac{P_{out}}{P_{in}} \quad (5)$$

Where $n$ is the rotational speed of the runner, $H$ is the net head, $Q$ is the flow rate, $N_j$ is the number of jets, $M$ is the torque measured on the turbine shaft, $\rho$ is the density of water and $g$ is the acceleration due to gravity.

## 3. Numerical Model

### *3.1. Physical Conditions*

It was noted by Perrig [5] that there are four flow regimes within a Pelton turbine system: i) confined steady-state flows in the upstream pipes and the distributor, ii) free jets past the injector, iii) transient free surface flow in the buckets and iv) dispersed 2-phase flow in the casing, which makes simulation of a full turbine a complex and demanding task. The flow in a Pelton casing is therefore by nature transient, multiphase and turbulent.

Once the water has left the runner the flow is guided to the tailrace by the casing walls and inserts. The flow is highly turbulent and mainly driven by inertia, however, since the Weber number is decreasing the water sheets tend to break up and droplet formation occurs. The kinetic energy is dissipated when the water sheets impact on a solid obstacle or when there is an intersection of one water sheet with another one, subsequently the flow is gravity driven.

### *3.2. Model Definition*

As mentioned previously, all simulations were carried out in FLUENT using the k-ε turbulence model and the VOF multiphase model at speed $n_{11} = 39$ and the best efficiency flow rate. Because of the complexity of the analysis, a preliminary in-depth study was carried out to evaluate the influence of the main numerical parameters on the stability of the simulation, in line with [6]. Based on previous studies in the literature [7] and in order to simplify the model, only half of the Pelton runner (through the plane of the bucket splitter) has been simulated and symmetry boundary conditions applied, shown in Figure 2.

The model consists of two domains, the stationary casing and rotating runner, where only six (out of the full 18) buckets have been modelled. The runner analysis is a transient simulation and the rotation is modelled using a sliding mesh approach, with an interface defined between the casing and runner domains. The meshes consisted of swept hexahedral cells within the stationary jet and a portion of the casing, highlighted in Figure 3 and fully tetrahedral cells within the runner domain. Face sizing was used to match the element size across the interface in order to minimise numerical diffusion error. Inflation layers were placed on all wall boundaries and the minimum wall distance was calculated to ensure agreement with the acceptable y+ limits for use with wall functions, i.e. $30 < y+ < 300$ [8].

Since computational time was a limiting factor for this project it was important to carry out a mesh sensitivity study to determine the effect the mesh size has on the appearance of casing flow, since it is known that an inadequate mesh sizing can smooth free surface interfaces and falsely modify flow features. Following a mesh independence study a mesh of 6.5 million cells was used and a conservative time step of 3.5219e-5 s, which equates to 0.2 degree rotation was chosen.

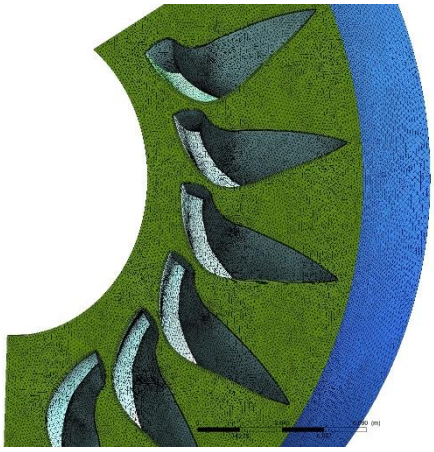

**Figure 2.** Runner mesh (fully unstructured).

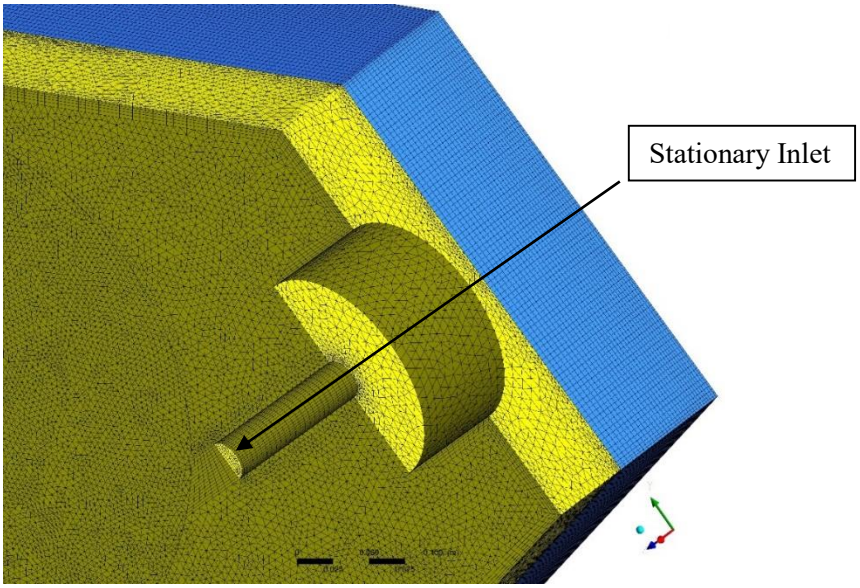


**Figure 3.** Casing mesh, showing structured (blue) and unstructured (yellow) regions.

It should be stated that it is not possible to make a quantitative prediction of the efficiency of a full Pelton turbine including the casing effects using the simulation described. However, the mesh validation was based on achieving a runner torque value independent of the mesh. In FLUENT a moment monitor is defined to measure the torque, which writes out the final value of the moment for each timestep. The work done by a single bucket is calculated through numerically integrating the torque curve using the trapezium rule to give the area under the total torque curve, multiplying this by the number of buckets gives the work done by the runner. The efficiency can then be obtained by dividing the work done by the hydraulic input power derived from the boundary conditions specification. Figure 4 compares the efficiency calculated from the mesh independent runner torque and the highest obtained experimental efficiency reported in this paper for upper jet. The error in the calculation is around 3%, this is slightly lower than the error orders of other numerical analyses carried out on Pelton turbines [6].

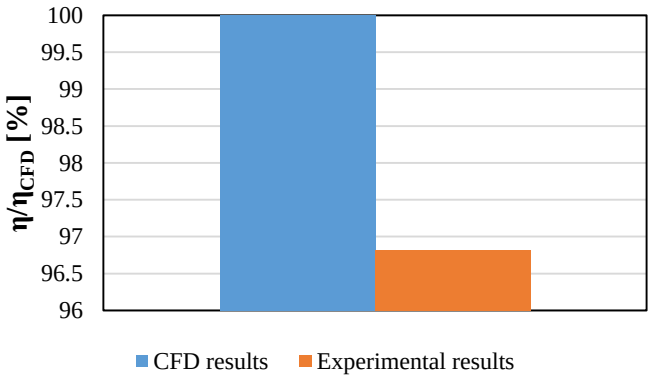


**Figure 4.** Comparison of the CFD and experimentally obtained efficiency.

*3.3. Casing Flow*

The first model simulated consisted of single jet operation of the upper injector for a standard width casing without internal shrouds or baffles. For post processing purposes, an isosurface of 1% water is

initially calculated. Since this is not physically realistic velocity vectors are plotted on the isosurface, coloured by magnitude (i.e. red high velocity and blue low velocity). Figure 5 shows a representative plot for the upper jet and is compared against a photograph of the experimental setup for the same operating point in Figure 6. The photograph is taken from the side window indicated in Figure 1. Identical black lines are overlaid in both Figure 5 and Figure 6, demonstrating good correlation of the CFD with the experimental result as both the direction and general shape of the water sheet as it impacts the front wall are captured. However, since it is only a snapshot it does not show the fully developed flow in the casing.

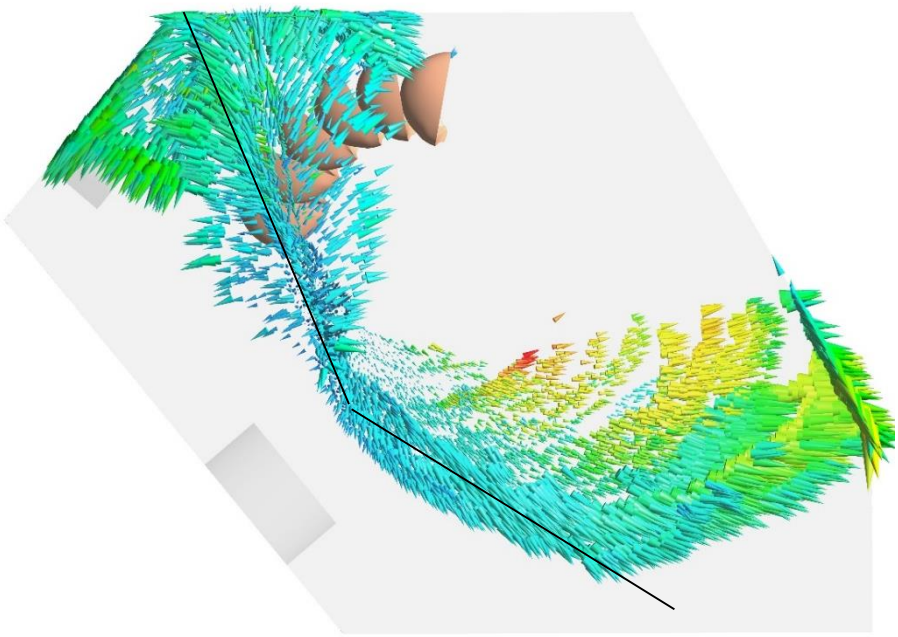

**Figure 5.** CFD velocity vectors upper jet.

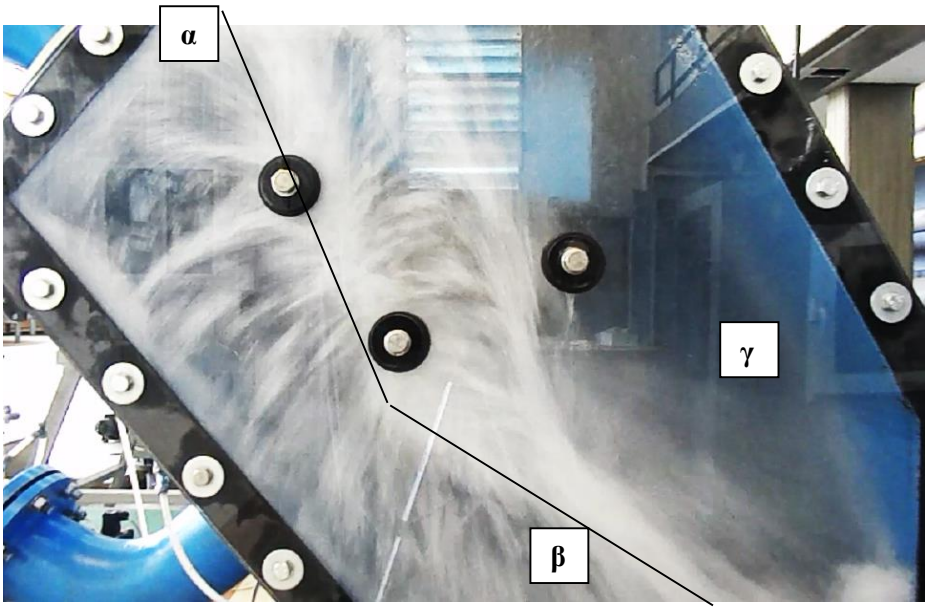


**Figure 6.** Experimental flow visualisation upper jet.

From Figure 6, three main portions of flow have been identified that offer visual comparison to the CFD results. These are documented in Figure 7, providing a more detailed description of the flow sequence as follows. The first, **α**, is the water that leaves closer to the root and along the sides of the bucket in the first 40° of rotation; this is shown in Figure 5 as the almost vertical water sheet. However, not all of the flow can leave the bucket in this first initial stage; the second portion of flow, **β**, leaves towards the middle of the bucket. This flow still has a remaining portion of axial kinetic energy and makes its way towards the front face of the casing below the runner closer to the tailrace. The third main portion, **γ**, is the last residual 20% of flow that remains in the bucket after at least 90° of rotation; this is mainly visible as a fine spray mist in the experimental visualisation that travels towards the symmetry plane as a result of high radial but low axial kinetic energy. Once the water has impacted the front face of the casing it dissipates much of its remaining kinetic energy and the major force is now gravitational, it spreads a short distance before falling into the tailrace below. However, on the side closest to the injectors this flow tends to recirculate and accumulate in the top left hand side of the casing, where interference with the water jet leaving the injectors occurs.

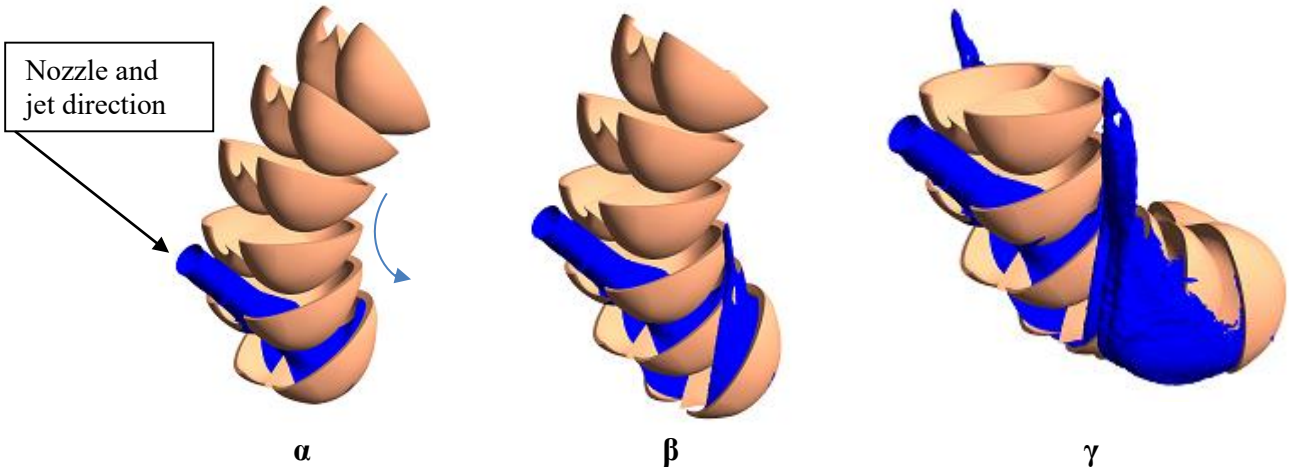


**Figure 7.** Flow Sequence.

Once the CFD model had been deemed suitable it was further applied to different designs (i.e. new meshes were generated with the same body, face and edge sizing). Similar to the upper jet comparison, Figure 8 shows the representative plot for the lower jet and is compared against a photograph of the experimental setup for the same operating point in Figure 9.

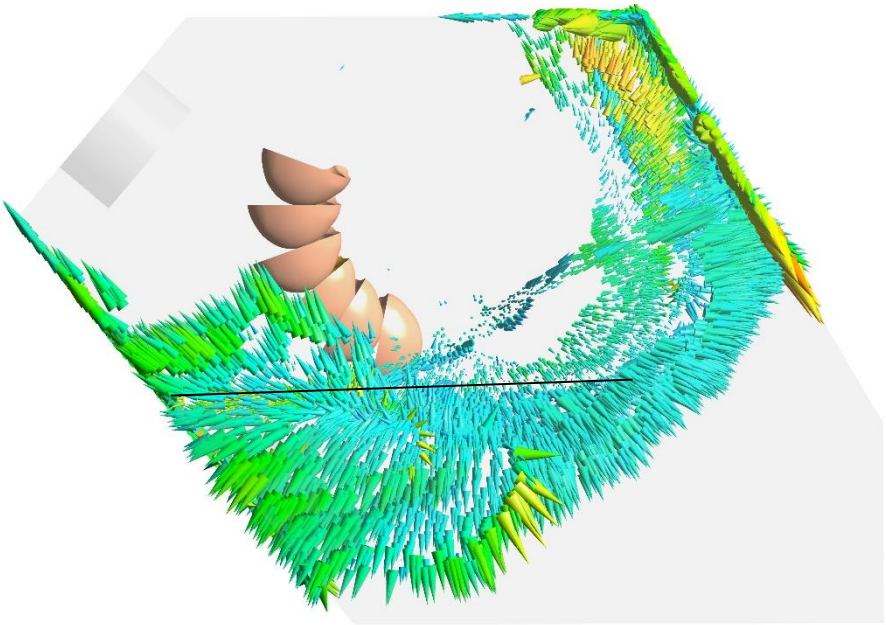

**Figure 8.** CFD velocity vectors lower jet.

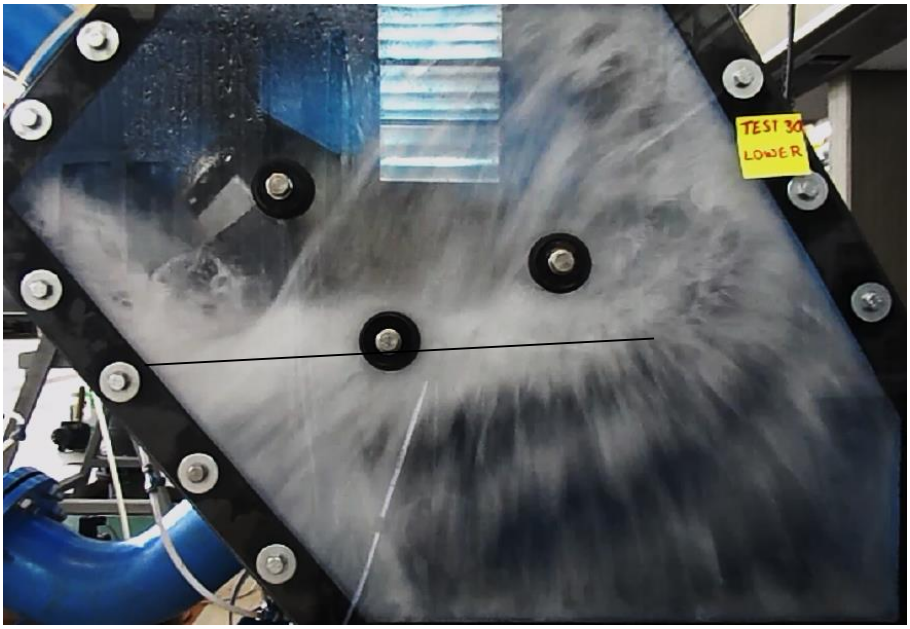


**Figure 9.** Experimental flow visualisation lower jet.

In the absence of shrouds or baffles the water is allowed to circulate around the casing. It can be noted from the velocity vectors in Figure 10(δ) that the water in the top left hand corner of the casing is directed towards the symmetry plane, eventually falling onto the injector and jet. Likewise, in Figure 10(ε), the water from the lower jet circulates in the top right hand corner before falling onto the runner. It is therefore recommended that a shroud be placed over the injectors and jet to ensure that the quality is not hindered by the splash water interference. Furthermore a curved baffle can be placed around the runner to inhibit water entering the roof of the casing, as recommended in [9].

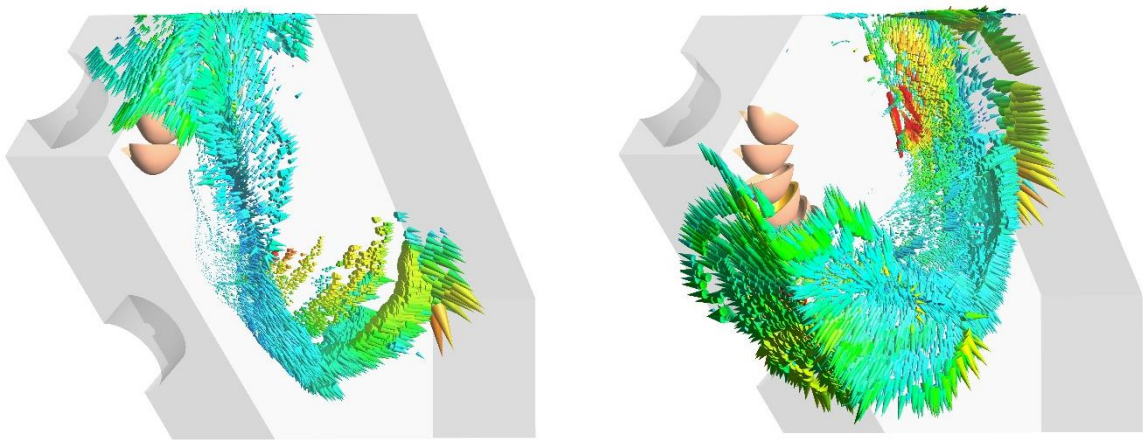

δ ε

**Figure 10.** Comparison of upper and lower injector.

In Figure 11 efficiency curves for the unit speed, $n_{11}$ = 39, are plotted against a range of non-dimensional flowrate, $Q_{11k}$, for both the upper jet and lower jet, with and without shrouding, normalised against the lower jet with shrouding, indicating the positive improvement of their installation, particularly at higher flow rates for the lower jet. While it is not yet possible to a make a quantitative prediction of the efficiency of a full Pelton turbine using the simulation described, it has nevertheless been shown by observations of the flow in the casing how baffles and shrouding can be added with positive effect. Since the addition of the curved baffle has very little influence on the flow for the upper jet, the corresponding photograph from experiment is shown for lower jet only in Figure 12.

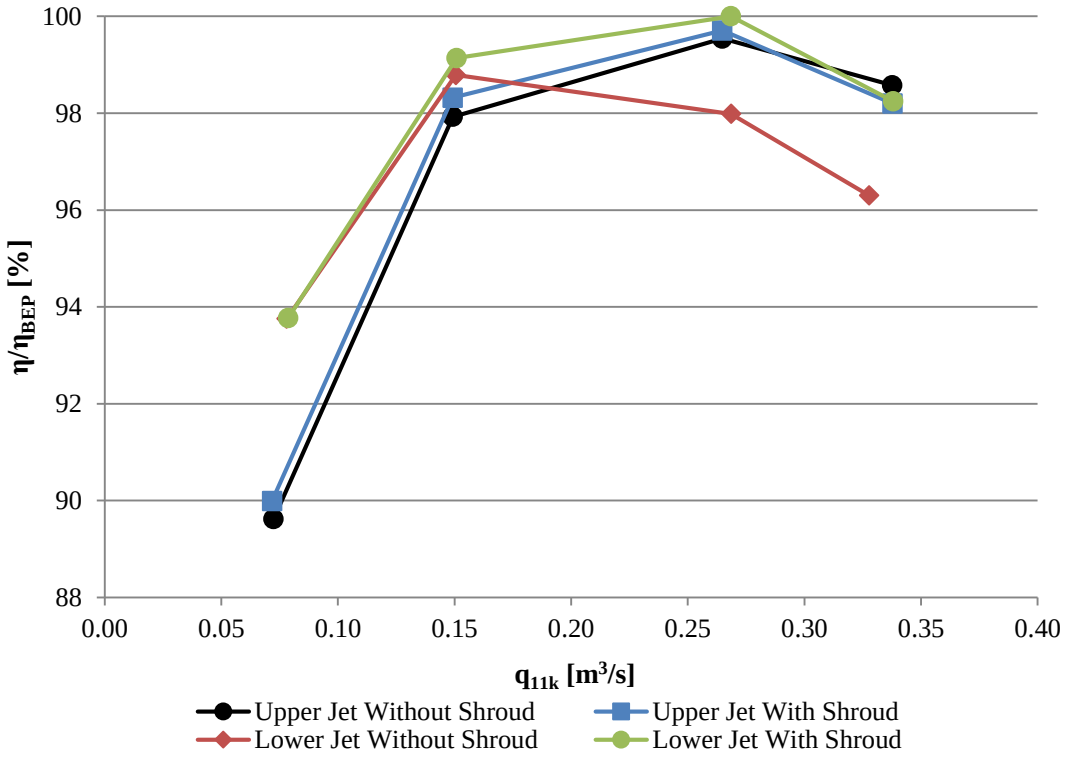


**Figure 11.** Comparison of experimental results for upper and lower injector with and without baffles and shrouds.

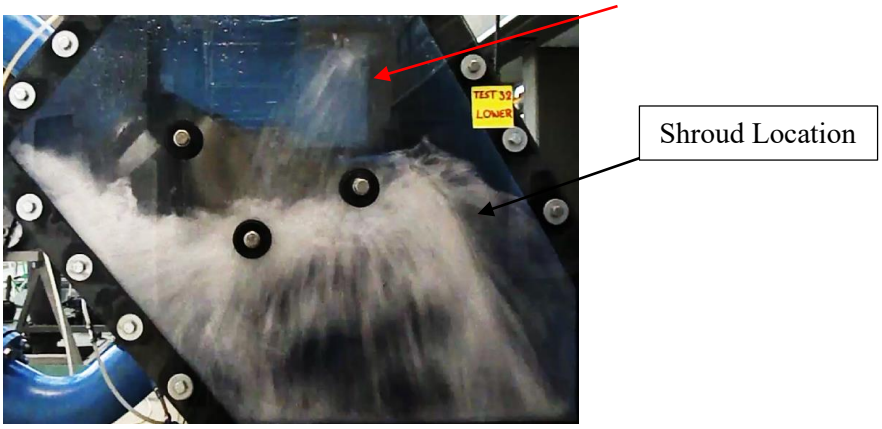


**Figure 12.** Lower jet with baffles and shrouds.

A small portion of flow still enters the roof of the casing, indicated by the red arrow. Therefore, the clearance between the baffle and the runner must be as small as possible to minimise the leakage through the clearance, which is created by the suction in the narrow gap which in turn leads to windage losses.

### *3.4. Further Investigation of Casing Design Parameters*

As previously mentioned very few design guidelines exist in the literature. However some sources [9] [10] [11] list generic dimensions, such as casing width, based on a ratio of bucket width or jet diameter. In this section the CFD model outlined in 3.2. will be used to further investigate the effect of casing width on turbine efficiency. Figure 13(σ) and Figure 13(ψ) compare the vector plots for the standard width and 45% of standard respectively for upper jet operation at the same time step. What is apparent is that the water has considerably higher kinetic energy in the narrower casing at the point it makes contact with the wall and therefore shows noticeably more spreading across the surface. Furthermore, due to the reduced width the water experiences a choking effect when it impacts the top corner, leading to considerable interference and further entrainment with the runner, resulting in higher windage losses, highlighted by the red arrow. In addition to testing the standard casing, and the 45% width a further two widths were considered. In order to carry out these experiments a number of panels separated by spacers into the Pelton test rig at NTUA. The upper jet efficiency curves for the unit speed, $n_{11} = 39$, are plotted against a range of non-dimensional flowrate, $Q_{11k}$, as shown in Figure 14.

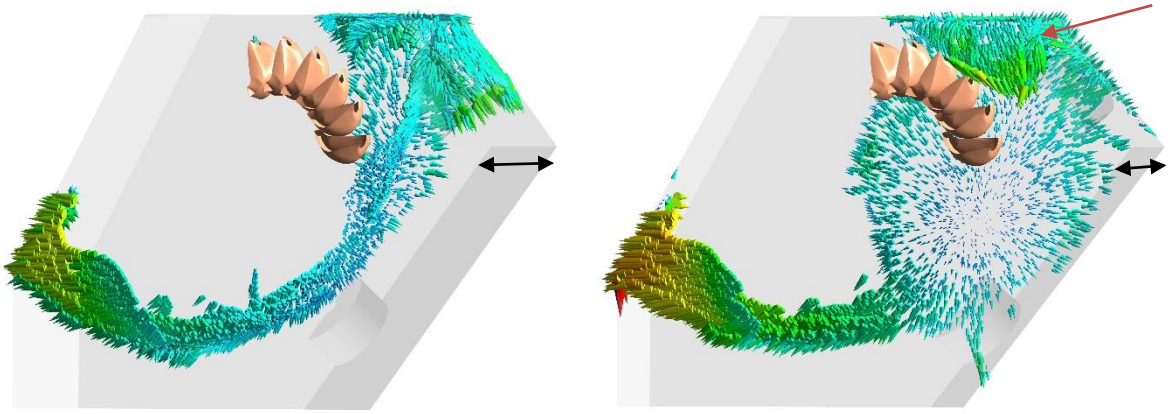

**σ** **ψ**

**Figure 13.** Comparing casing width (black arrows indicating relative width).

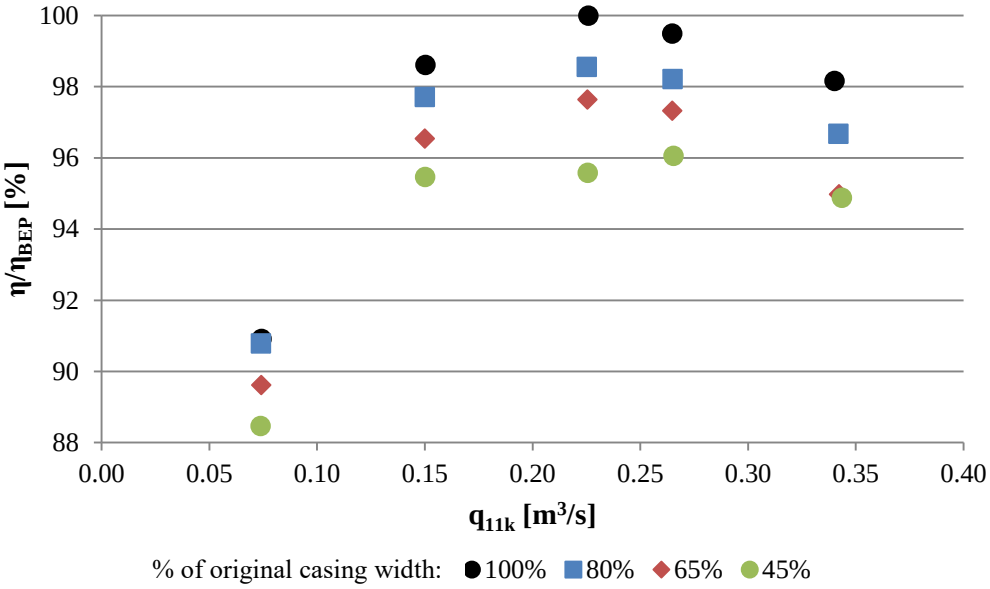


**Figure 14.** Pelton experimental efficiency curves showing effect of casing width at $n_{11}$=39.

Since these tests were equipped with the same baffles and shrouds described in 3.3 it is evident that the overall dimensions of the casing have much larger effect on efficiency than the gain made by the addition of the baffle and shrouds.

## 4. Conclusions

This paper has presented how the FLUENT CFD code can be used to simulate flow within the casing of Pelton turbines. Despite good visual correlation it is not yet possible to obtain a quantitative measure of efficiency using the presented method, therefore experimental model testing is required to ascertain improvements from the suggested design changes. One of the key disadvantages of this method is the long simulation timescales, which makes it unfeasible to compare results from a range of designs. Moreover, to obtain high fidelity models a denser mesh, smaller time step and higher order discretisation methods, than those initially chosen would be required. Accordingly, compromises have to be made, which introduce numerical errors that falsely modify the flow features.

Nevertheless, the CFD model has been shown to be a good predictor of casing flow, such that a number of baffles and shrouds were proposed, which had a positive impact on performance. Furthermore, casing width has been investigated and it was found that there appears to be a linear relationship with efficiency and that casing dimensions have a greater overall impact on efficiency than the addition of baffles and shrouds.

It is envisaged that with time CFD modelling of Pelton turbines will continue to improve, however as yet it still can only be used as a design tool to make predictive improvements to casing design.

## Acknowledgements

The authors would like to thank Gilbert Gilkes & Gordon Ltd, Lancaster University Renewable Energy and Fluid Machinery Group and the Laboratory of Hydraulic Turbomachines, NTUA.

## References

[1] Staubli T, Weibel P, Bissel C, Karakolcu A and Bleiker U 2010 Efficiency increase by jet quality improvement and reduction of splashing water in the casing of Pelton turbine *16th Int. Seminar on Hydropower Plants*

[2] Neuhauser M, Leboeuf F, Marongiu J C, Parkinson E and Robb D 2012 Simulations of Rotor-Stator Interactions with SPH-ALE in *Advances in Hydroinformatics: SIMHYDRO 2012 - New Frontiers of Simulation* (Singapore: Springer Hydrogeology)

[3] Rentschler M, Neuhauser M, Marongiu J C and Parkinson E 2016 Understanding casing flow in Pelton turbines by numerical simulation *IOP Conf. Ser.: Earth Environ. Sci.* **49** 022004

[4] International Electrotechnical Commission 1999 *IEC 60193: Hydraulic turbines, storage pumps and pump-turbines - Model acceptance tests* (Geneva: IEC)

[5] Perrig A 2007 *Hydrodynamics of the Free Surface Flow in Pelton Turbine Buckets* PhD Thesis (Lausanne: EPFL)

[6] Santolin A, Cavazzini G, Ardizzon G and Pavesi G 2009 Numerical investigation of the interaction between jet and bucket in a Pelton turbine *Proc. IMechE Vol. 223 Part A: J. Power and Energy* **223** 721-8

[7] Gupta V, Prasad V and Khare R 2016 Numerical simulation of six jet Pelton turbine model *Energy* **104** 24-32

[8] Launder B E and Spalding D B 1974 The Numerical Computation of Turbulent Flows *Computer Methods in Applied Mechanics and Engineering* **3** 269-289

[9] Nechleba M 1957 *Hydraulic Turbines: Their Design and Equipment* (Prague: Artia)

[10] Quartz L and Meerwarth K 1963 *Wasserkraftmaschinen: Eine Einführung in Wesen, Bau und Berechnung von Wasserkraftmaschinen und Wasserkraftanlagen* (Berlin und Heidelberg: Springer-Verlag)

[11] Raabe J 1970 *Hydraulische Maschinen und Anlagen. Teil 2 Wasserturbinen* (Düsseldorf: VDI-Verlag)